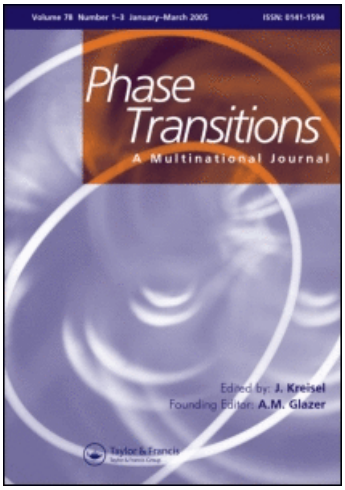

Phase Transitions
Publication details, including instructions for authors and subscription information:
http://www.informaworld.com/smpp/title~content=t713647403

Phase behavior of dispersions of hard spherical particles

W. Van Megen[a]; P. N. Pusey[b]; P. Bartlett[c]
[a] Department of Applied Physics, Royal Melbourne Institute of Technology, Melbourne, Victoria, Australia [b] Royal Signals and Radar Establishment, Malvern, Worcestershire, England [c] School of Chemistry, University of Bristol, Bristol, England

To cite this Article Van Megen, W. , Pusey, P. N. and Bartlett, P.(1990) 'Phase behavior of dispersions of hard spherical particles', Phase Transitions, 21: 2, 207 — 227
To link to this Article: DOI: 10.1080/01411599008206892
URL: http://dx.doi.org/10.1080/01411599008206892

Phase Transitions, 1990, Vol. 21, pp. 207–227
Reprints available directly from the publisher
Photocopying permitted by license only

PHASE BEHAVIOR OF DISPERSIONS OF HARD SPHERICAL PARTICLES

W. VAN MEGEN

Department of Applied Physics,
Royal Melbourne Institute of Technology,
Melbourne, Victoria, 3000, Australia.

P. N. PUSEY
Royal Signals and Radar Establishment,
Malvern, Worcestershire, WR14 3PS, England.

and

P. BARTLETT
School of Chemistry,
University of Bristol,
Cantock's Close, Bristol, BS8 ITS, England.

(Received 1 June 1989; in final form 20 September 1989)

A series of experiments on concentrated dispersions of hard colloidal spheres is discussed. The observed phase behavior is analogous to that of simple atomic systems: colloidal fluid, crystal and glass phases are found. The structure of the crystals, revealed by light diffraction, is a strongly faulted stacking of hexagonally-packed layers of particles. Dynamic light scattering confirms that the concentration of the metastable fluid phase for which long-ranged particle diffusion ceases coincides with the concentration where the glass transition is observed macroscopically. In studies of a binary mixture of colloidal spheres with a size ratio 0.61 eutectics, glass formation and the AB_{13} type alloy structure have been identified.

KEY WORDS: Phase transitions, hard spheres, light scattering, concentrated dispersions, mixtures, glass transition.

1 INTRODUCTION

A fascinating property of colloidal dispersions is their ability to form structures or arrangements of particles with a periodicity comparable to the wavelength of visible light. Bragg reflection of light from these structures provides the beautiful colorful appearance of naturally-occurring colloids, such as gem opals, and synthetic colloids, such as dialyzed concentrated dispersions of polystyrene latex spheres. Two-dimensional ordering and the coexistence of ordered and disordered phases in dispersions of rod-shaped (tobacco mosaic virus and vanadium pentoxide) and disc-shaped (bentonite) particles were reported in the 1930's. An extensive presentation of these

observations was given by Langmuir in 1938. In 1957 it was established that particles of tipula iridescent virus, which have the shape of icosahedra, could form crystals showing three-dimensional order (Williams and Smith, 1957); a study by light scattering crystallography of the structure of these crystals was reported subsequently (Klug, Franklin and Humphreys-Owen, 1959). Nearly monodisperse polymer colloidal spheres were first synthesized in 1947. Some years later it was shown that these particles also form colloidal crystals and a number of studies of their optical properties was reported (Alfrey *et al.*, 1954; Luck, Klier and Wesslau, 1963; Krieger and O'Neill, 1968; Hiltner and Krieger, 1969).

The analogy between the behavior of colloidal particles in dispersion and simple atomic or molecular materials was implicit in the early work of Einstein (1905–1911), Constantin (1914) and Perrin (1914). This analogy was subsequently placed on a firm statistical mechanical basis by McMillan and Mayer (1945) and Kirkwood and Buff (1951). Once the solvent-averaged potential of mean force among the dispersed particles is identified, the thermodynamic properties of a dispersion are formally equivalent to those of an atomic fluid with the same inter-atomic potential. Then statistical mechanics, combined with well-established theories of the liquid and solid states, can be used to calculate such properties as structure, phase behavior and the equation of state (van Megen and Snook, 1984). In this thermodynamic sense, a dispersion of identical colloidal spheres can be regarded as a one-component assembly of "super-atoms". However, while we will not emphasize it in this paper, it is worth mentioning that the dynamic properties of colloids in dispersion are generally different from those of atoms (although, even here, intriguing similarities can be found (Hess and Klein, 1983; Tough *et al*, 1986)).

In this paper we describe properties of concentrated dispersions of poly-(methylmethacrylate) particles stabilized by a relatively thin steric barrier. The dispersions are made transparent, and therefore suitable for optical studies and direct observation, by nearly matching the refractive index of the two-component suspension liquid to that of the particles. This index matching has the added advantage of minimizing van der Waals attractions between the particles. To a good approximation the interparticle interaction in these dispersions appears to be "hard-sphere".

Assemblies of hard spheres play an important role in statistical physics as models for simple liquids (Hansen and McDonald, 1976); they constitute what is probably the simplest system to show a freezing/melting transition. However hard-spherical atoms do not exist in reality. A major thrust of our recent work has been to interpret data obtained on these colloidal dispersions in terms of theories and computer simulations applied originally to the hypothetical hard-sphere atomic system. When viewed as an assembly of hard spheres the colloidal system has several useful properties. In principle, at least, the particle size can be varied over a wide range allowing, for example, precise choice of size ratio in the study of binary mixtures. The diffusive motions of near-micron sized particles in dispersion are many orders of magnitude slower than those of atoms. The consequent very slow structural relaxation times of concentrated dispersions allow one to prepare and study metastable fluid and glassy phases and to follow the time evolution of crystallization (Pusey and van Megen, 1987a,b).

In the next section we describe the particles and the preparation of samples. The phase behavior of the system is considered in Section 3; with increasing particle concentration we identify fluid, crystalline and glassy structures. In Section 4 we describe the determination of the crystal structure by "powder" light-scattering crystallography; we find a close-packed structure with a high degree of faulting in the stacking of the crystal planes. Section 5 deals with a study, by dynamic light scattering, of the divergence of the structural relaxation time of the metastable colloidal fluid as the glass transition is approached. Finally in Section 6 we review briefly some recent studies of a binary mixture of different sized particles.

Most of the work to be described has been, or will be, published elsewhere. Here we give a general overview, omitting unnecessary detail.

2 SAMPLE PREPARATION

The particles used in this work were prepared by the polymerization of methylmethacrylate in an organic liquid in the presence of a preformed stabilizer comprising a "comb" of poly-(12-hydroxystearic acid) (phsa) on a poly-(methylmethacrylate) (pmma) backbone. Details of this preparation are documented elsewhere (Antl *et al.*, 1986). The polymerization process is followed by a "locking" stage, which chemically grafts the pmma backbone of the stabilizer onto the particle, and appropriate "cleaning" procedures. The resulting stock dispersion consists of pmma particles of approximately predetermined radius stabilized by a layer of phsa of 10–15 nm thickness dispersed in an organic liquid, decalin in our case. The coefficient of variation of the particle radii, or polydispersity, was less than 0.05. Both this quantity and the average particle (hydrodynamic) radius were determined by dynamic light scattering on dilute samples.

Although the difference between the refractive indices (n) of the pmma particles ($n \simeq 1.50$) and decalin ($n \simeq 1.48$) is small, near micron sized particles scatter visible light so strongly that, except at extreme dilution, the dispersions are opaque. Thus, the behavior in the bulk of the samples cannot, in general, be studied with visible light. We overcome this difficulty by adding the amount of carbon disulfide ($n \simeq 1.63$) that provides (nearly) transparent dispersions. The resulting optically matched dispersions, prepared in cells of square (1 cm^2) cross-section, can be brought to the required particle concentration by centrifuging at about 1000 g until a compact sediment forms, decanting a weighed amount of clear supernatant, then redispersing the particles by agitation of the sample.

There is considerable evidence that some CS_2 is absorbed initially by the pmma particles (Ottewill and Livsey, 1987; van Megen and Underwood, 1989). However, the increase in particle radius in the refractive index matching CS_2/decalin mixture, relative to that in pure decalin, is only a few percent. More significantly, the presence of CS_2 does not appear to alter the nearly hard-sphere form of the interparticle forces. As discussed in the following section, difficulties associated with uncertainties in the precise chemical compositions of the particles and liquid medium, due to this CS_2

absorption, are essentially circumvented by expressing the dispersion volume fractions in terms of effective hard sphere volume fractions.

3 PHASE BEHAVIOR

In this section we discuss a study of the phase behavior of dispersions of pmma particles of radius, $R = 325$ nm Pusey and van Megen, 1986, 1987a. Nine samples at different concentrations were prepared by the procedure described in the previous section.

Since colloidal solids are weak (Chaikin *et al.*, 1987) slow tumbling (at about 1 rev/s) of the samples imposes shear stresses sufficiently large to destroy any crystalline structures that may be present. Randomization of the particle positions in the dispersions is evident from their amorphous appearance after tumbling. Tumbled samples, labelled 2 to 10, were arranged in increasing order of concentration, illuminated by white light and left undisturbed for observation over several days.

Within hours small Bragg-reflecting crystals were evident throughout the dispersion in samples 3 to 7. It is important to emphasize that these crystallites formed *without* the aid of added nuclei. We can, therefore, describe this process as "homogeneously nucleated crystallization" as distinct from "heterogeneously nucleated crystallization", discussed below, which requires the assistance of a nucleating surface.

The particles are slightly denser than the liquid. This, combined with the fact that the particles become more closely packed upon crystallization, causes gradual gravitational settling of the crystallites in samples 3 to 5 until, after about 24 hours, a distinct boundary appears that separates crystalline and disordered phases (see Plate 1). However, overall gravitational settling of the particles individually is very much slower and is only significant after 4 or 5 days. The crystallites in these samples appear randomly orientated and have linear dimensions of about 50 μm. The upper phase in samples 3 to 5 is disordered or fluid-like; the large particle concentration imposes significant short-ranged spatial correlation between the particles, but the amorphous appearance indicates the absence of long-ranged order (see Plate 1). These features are quantitatively represented by the static structure factor, discussed in the next section. In samples 6 and 7, the entire volumes are occupied by similar, but smaller, crystallites and even after 4 days, there is no evidence of their settling or phase separation.

The height of the phase boundary, in samples 3 to 5, stabilized after 2 days and we assume that at this stage the boundary separated coexisting crystalline and fluid-like phases in equilibrium. Accordingly, for these samples, the proportion of crystallites was plotted as a function of the weight fraction of pmma (see Figure 1). Extrapolation of the resulting straight line to zero and 100 % crystals then provides the weight fractions at which crystallization (freezing) and melting occur. The hard-sphere model is now invoked by equating the weight fraction of the dispersion at freezing with the volume fraction $\phi_F = 0.494$, obtained from computer simulation for the freezing of a hard-sphere fluid (Hoover and Ree, 1968). The weight fractions of the other samples are converted accordingly and their concentrations will henceforth be expressed as effective hard-sphere volume fractions, ϕ. The melting volume

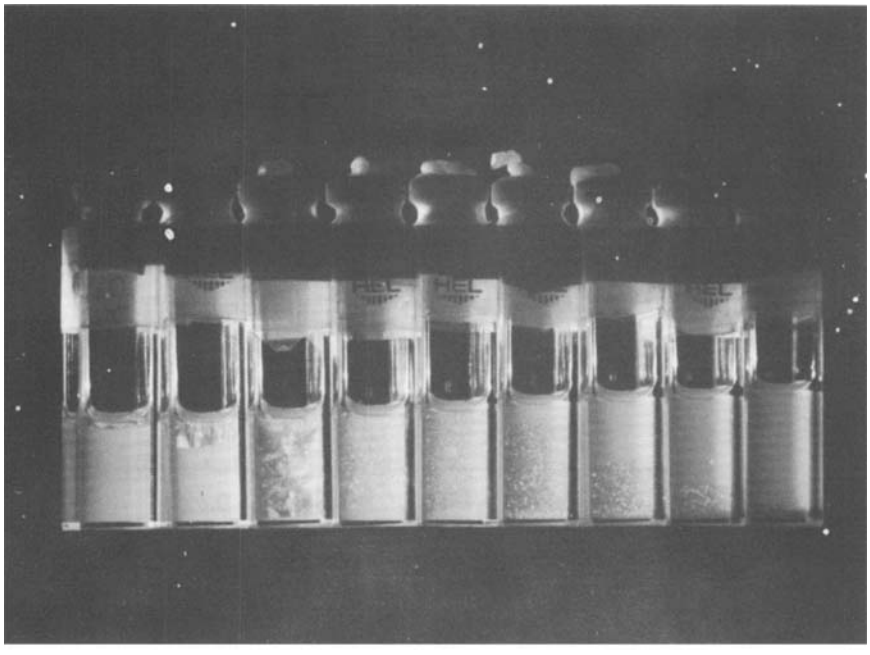

(a)

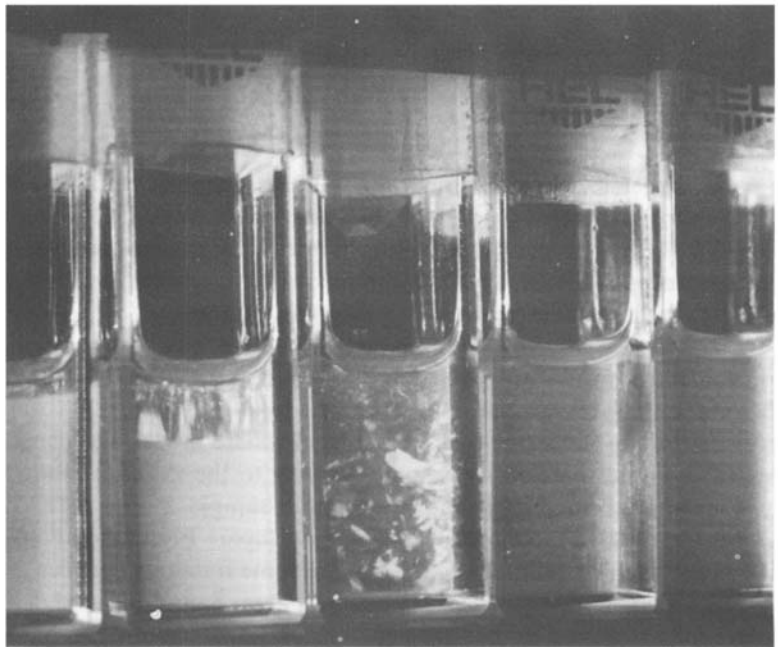

(b)

Plate 1 (See Color Plate XIII at the back of this publication.) (a) View of the samples illuminated obliquely from behind, numbered 2 to 10 from the right, in order of increasing volume fractions. Actual effective hard sphere volume fractions are indicated in Figure 1. (b) Close-up of samples 7 to 9. The middle sample (8) is completely occupied by large heterogeneously nucleated crystals. At higher volume fractions, the samples are mainly amorphous.

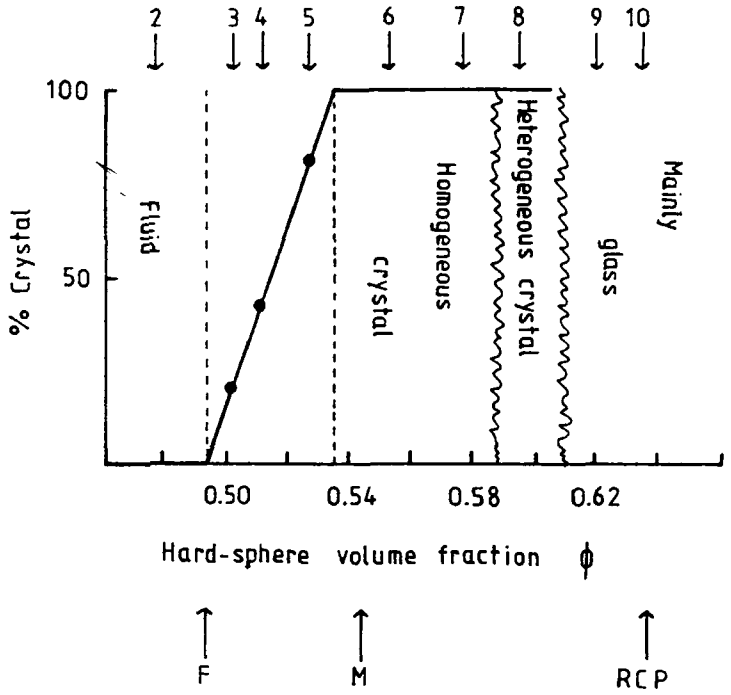

Figure 1 Phase diagram of hard-sphere colloidal dispersions. Arrows at the top indicate the effective hard-sphere volume fractions of the dispersions of the 325 nm radius pmma particles. Arrows at the bottom indicate the freezing, melting and random close-packed volume fractions known for hard spheres.

fraction of the dispersion thus obtained, $\phi_M = 0.536$, is slightly below the theoretical value of 0.545 for the melting point of the hard sphere crystal (Hoover and Ree, 1968). The difference between these values is probably within experimental error, although the small polydispersity of the samples or the slight departure of the actual interparticle particle potential from the hard-sphere interaction could also be responsible for a slightly lower melting volume fraction. This way of stating the particle concentration has a firm thermodynamic basis and avoids the need to specify the exact chemical composition of the particle and adsorbed layer.

We now discuss, in the framework of the hard-sphere model, the phase behavior (summarised in Figure 1) of all the samples leading to the situation, shown in Plate 1, taken 4 days after tumbling. The most dilute sample 2, $\phi = 0.477$ (i.e. below freezing) did not show any sign of crystallization (apart from a small sedimentary crystal, discussed below). Samples 3 to 5 have volume fractions between ϕ_F and ϕ_M and show increasing proportions of crystalline phase. Samples 6 and 7 (both with $\phi > \phi_M$) are fully occupied by homogeneously nucleated crystals. On increasing the volume fraction beyond ϕ_M the thermodynamic driving force for crystallization increases. This results in larger concentrations of nuclei and the ultimate formation of smaller crystals as can be seen in Plate 1 by comparing the size of the crystals in samples 3 to 5 with those in samples 6 and 7.

However, the reduction of the particle mobility (or increase in viscosity of the dispersion) with increasing ϕ, leads to progressively longer crystallization, or structural relaxation, times. In fact sample 8 ($\phi = 0.596$) is unable to crystallize homogeneously and undergoes a much slower epitaxial crystallization which is nucleated heterogeneously at the meniscus and cell walls. In the most concentrated samples 9 and 10 (with $\phi = 0.620$ and 0.636, respectively) the loss of particle mobility is so severe that after several days only some crystallization was evident at the meniscus (see Plate 1). However, even after many months these samples were still predominantly amorphous. We therefore designate the state of those samples with $\phi > \phi_g \simeq 0.60$ which fail to crystallize fully as "colloidal glass". It is interesting that the volume fraction of sample 10, $\phi = 0.636$ is very similar to the value 0.64 found by Bernal for the random close packing of hard spheres.

The appearance of the samples after 4 days, shown in Plate 1, warrants further comment. As mentioned above, gravitational settling of the particles, a much slower process than the crystallization discussed above, also occurs. After about 4 days this is evident at the bottom of the most dilute sample by the formation of sedimentary crystals. In the lower region of samples 3 to 7, gravitationally compacted crystals are evident from the Bragg reflections at shorter wavelengths (giving rise to the predominantly greenish appearance). We suggest two possible mechanisms for the partial crystallization of samples 9 and 10. As mentioned above, these samples showed no sign of any crystallization for 2 to 3 days. One possibility is that the slight settling of particles over this time reduced the concentration near the meniscus to the point where crystallization was nucleated. Alternatively, ordering could be induced by the shear associated with the weak flows which could persist for a considerable period after tumbling these very viscous samples. This crystallization then proceeded downwards until it stopped in a region of higher concentration.

The phase behavior displayed in Plate 1 (and summarized in Figure 1) illustrates an advantage of dispersions of near micron sized particles over atomic systems as model fluids; the structure, in particular the difference between disordered and crystalline phases, can be seen directly. However, the visual similarity of the disordered phase in samples 2 to 5 and the amorphous portions of samples 9 and 10 disguises very significant differences in the dynamic properties of the equilibrium fluid-like phase and the long-lived metastable glass phase. For example, the shear viscosity of samples 9 and 10 is about five orders of magnitude larger than that of the disordered dispersions in samples 2 to 5. The large viscosity of the higher volume fraction dispersions is a manifestation of the very small mobility of the particles. For $\phi > \phi_g$, the mobility is so small that the structural rearrangements required for crystallization of the metastable amorphous state do not occur on an experimentally accessible time scale. Dynamic light scattering results, presented in Section 5, show a close correspondence between the volume fraction at which the dispersion no longer crystallizes and that where the structural relaxation times become essentially infinite.

From the discussion of Section 1 it should be apparent that the freezing transition exhibited in Figure 1, is similar in nature to the fluid–solid transition expected in a supercritical atomic material (see, for example, Egelstaff, 1967). (At temperatures well above the critical temperature any attractive part in the inter-atomic potential has

little effect on the material properties). An important difference in the usual experimental studies of colloidal and atomic systems is the following: A monodisperse colloidal dispersion is effectively a one-component system of interacting particles in an inert incompressible liquid medium. Studies are usually made at constant *volume* (or volume fraction) and temperature. Thus, as we have seen, when a volume fraction between ϕ_F and ϕ_M is chosen an initially metastable dispersion will separate into an equilibrium state composed of coexisting colloidal fluid and colloidal crystal phases; the osmotic pressure of the dispersion (the analogue of the pressure in an atomic system) will adjust itself to the value required by the equation of state. By contrast, atomic systems are frequently studied at constant *pressure* and temperature. Then phase coexistence is essentially impossible to achieve since the temperature cannot be set precisely and will, in practice, be slightly above or slightly below the melting temperature at the pressure chosen. At constant pressure and temperature, therefore, the practically-achieved equilibrium state of the system will be a single-phase solid or fluid.

4 THE CRYSTAL STRUCTURE

In these colloidal suspensions the naturally-occurring homogeneously-nucleated crystallization process provides samples composed of many small randomly-oriented crystallites which are ideal for the light scattering equivalent of powder crystallography. For materials composed of N identical spheres which are in an orientationally-invariant state such as a fluid or a powder of crystallites the intensity of scattered light can be written

$$I(q) = P(q)S(q) \tag{1}$$

where the magnitude of the scattering vector $\mathbf{q}$ is defined by

$$q = \frac{4\pi}{\lambda} \sin \frac{\theta}{2}. \tag{2}$$

λ is the wavelength of the light in the dispersion and θ the scattering angle; $P(q)$ is the single-particle form factor, determined by the refractive index profile of the particles, and $S(q)$ is the static structure factor defined by

$$S(q) = N^{-1} \sum_{j=1}^{N} \sum_{k=1}^{N} \langle \exp[i\mathbf{q} \cdot (\mathbf{r}_j - \mathbf{r}_k)] \rangle, \tag{3}$$

where $\mathbf{r}_j$ is the position of particle j. The particle form factor $P(q)$ can be obtained by measuring $I(q)$ for a dilute dispersion (for which $S(q) = 1$). For the pmma particles we find $P(q)$ to have the form expected for spherically-symmetric core/shell objects which generally show strong scattering at small q and weak subsidiary maxima at larger q. The structure factor (in arbitrary units) of a concentrated sample is obtained by measuring $I(q)$ and dividing by the $P(q)$ measured on the dilute suspension.

To make the powder diffraction measurements a laser beam was expanded so that about 1 cm^3 of the sample, containing at least 10^6 crystallites, was illuminated (Pusey

et al., 1989). A photomultiplier tube, preceded by suitable optics, rotated about the axis of the cell under computer control. Angular scans from 20° to 140°, in steps of 0.25°, took about 10 min.

Figure 2 shows structure factors obtained from a sample of spheres of radius 170 nm at a concentration just above melting (the phase behavior of this system of particles will be described in the next section). The lower curve was measured immediately after the sample had been mixed well by slow tumbling. It has the general form expected for a metastable fluid. The upper curve was obtained about 80 minutes later when the sample appeared to be fully crystalline. The form of this structure factor is rather unusual for a crystal in that, in addition to a sharp Bragg reflection, a broader band of diffuse scattering is evident. Furthermore this diffuse scattering has approximately the same amplitude as the structure factor of the metastable fluid, indicating that it must arise from short-ranged rather than long-ranged order.

To interpret this result we speculate on possible crystal structures. It is generally expected that the structure of crystals formed by particles with short-ranged isotropic interactions should be close packed. As is well-known, close-packed structures can be made by stacking hexagonally-packed layers of particles (Guinier, 1963). Each layer can take one of three lateral positions, A, the reference position, B, obtained by an in-plane displacement relative to A of $1/3\mathbf{a} + 2/3\mathbf{b}$ and C obtained by the displacement $2/3\mathbf{a} + 1/3\mathbf{b}$, where a and b are hexagonal lattice vectors in the planes.

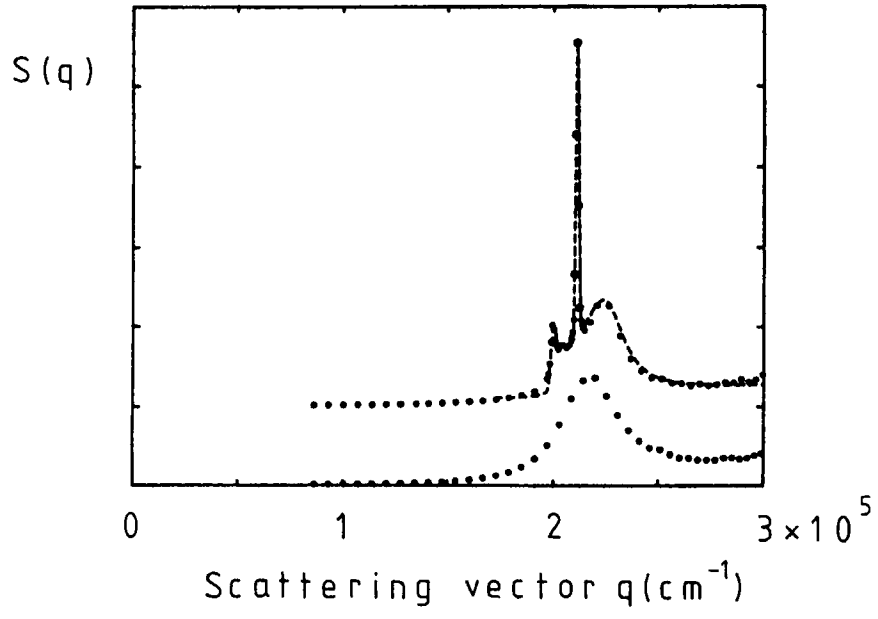

Figure 2 Structure factors (in arbitrary units) for the dispersion of 170 nm radius pmma particles at $\phi = 0.54$, i.e. just above melting. The lower result applies to the metastable fluid, the upper result, shifted up one division for clarity, to the crystalline phase. The dashed solid line represents the theoretical result, as discussed in the text.

The sequences .. ABABAB .. gives a hexagonal close-packed (HCP) structure whereas .. ABCABC .. gives face-centred-cubic (FCC). However, the only essential requirement for close packing is that adjacent layers, n and $n + 1$, have different positions. For hard spheres there seems no reason to expect much "communication" between layers n and $n + 2$. We therefore postulate that hard spheres may adopt a randomly-stacked sequence such as .. ABACBCA ... For generality we assign a probability α that layers n and $n + 2$ have different positions. Thus $\alpha = 0$ gives HCP and $\alpha = 1$ FCC.

Calculation of the powder diffraction pattern of a crystal comprises two steps, determination of its structure in reciprocal space and orientational averaging (Guinier, 1963). The reciprocal-space structure of a close-packed crystal, random-stacked in the sense described above, was calculated many years ago (Hendricks and Teller, 1942; Wilson, 1942, 1949). It contains points, which give rise to those Bragg reflections in real space that are common to both HCP and FCC structures, and modulated lines resulting from the random stacking, which provide broad bands of diffuse scattering. The nature of the modulation of these lines, and therefore the form of the diffuse bands in the structure factor, depends on the stacking probability α. When reciprocal space contains such lines the orientational-averaging procedure involves subtleties not found in the case of a perfect crystal; these are discussed elsewhere (Pusey *et al.*, 1989).

We have calculated powder diffraction patterns for a range of values of α. Other adjustable parameters are an overall scaling factor and the average dimensions of the crystallites perpendicular and parallel to the close-packed planes; the latter determine the diffraction-broadening of the pattern. We should emphasize that the term "close-packing" is used above to characterize the average spatial arrangement of the particles. It does not imply that the particles are necessarily touching. In fact, the volume fraction, $\phi_M = 0.545$, of the hard sphere crystal at melting is well below the volume fraction, 0.74, of touching close packing. Thus particles in a crystal at $\phi \simeq \phi_M$ have significant freedom for Brownian motion about their lattice sites which will give rise to thermal diffuse scattering and reduction of the Bragg reflections by the Debye–Waller factor. We have included thermal motion in the calculations by assuming a simple Einstein (independent oscillator) model of the crystal and taking the mean-square displacement of the particles about their lattice sites to be that found in computer simulations of hard spheres (Young and Alder, 1974).

The dashed line in Figure 2 is the powder pattern for $\alpha = 0.5$, calculated by the procedure just described. It agrees well with the experimental data. We conclude, therefore, that the crystal structure of this sample is completely random-stacked in the sense that following an AB stacking of two layers, positions A and C of a third layer are equally likely.

Elsewhere (Pusey *et al.*, 1989) we have published diffraction patterns of two other samples of the same particles. In one case the concentration was somewhat lower, between ϕ_F and ϕ_M. At this reduced "supersaturation" the sample took longer, about a day, to show complete crystallization and phase separation. The diffraction pattern of the polycrystalline phase could be fitted by that calculated by the procedure described above but now with $\alpha = 0.58$. The second sample contained a crystal

formed over several weeks by sedimentation of particles from a relatively dilute, $\phi \simeq 0.25$, suspension. Then $\alpha \simeq 0.8$ was required to describe the structure factor.

Thus there appears to be a correlation between the rate at which the crystals are formed and a tendency to show increasingly longer sequences of FCC stacking, $\alpha \to 1$. We might conjecture therefore that the true equilibrium state of a hard-sphere crystal is FCC but that the difference in free energies between this and other close-packed structures is small. When the crystal is grown slowly the particles have more time to explore possible sites on the faces of the crystallite and to achieve the equilibrium state. By contrast, on rapid growth, long-lived, but strictly non-equilibrium, states can be formed.

Indeed several calculations have indicated that the free energy of the FCC hard-sphere crystal is slightly lower than that of the HCP structure (Frenkel and Ladd, 1984; Colot and Baus, 1985; Igloi, 1986); however, the difference is comparable to error in the calculations.

To our knowledge, while a significant degree of faulted stacking can be found near a structural phase transition, (Edwards and Lipson, 1942), no simple atomic material shows the essentially complete stacking randomness observed in Figure 2. Faulted stacking in crystals of colloids was considered previously by Sanders (1968) who showed that the resulting diffuse scattering plays an important role in determining the optical quality of gem opals.

5 PARTICLE DYNAMICS AROUND THE GLASS TRANSITION

In Section 3 we showed that dispersions can be concentrated to a metastable state that for $\phi > \phi_g$, remains amorphous for an essentially indefinite period. This property is a consequence of the slow translational diffusive motion of the near micron-sized particles in the dispersions. However, even at lower volume fractions ($\phi_F < \phi < \phi_g$), the structural relaxation times are sufficiently large to allow observation of the metastable states that exist after tumbling the dispersions but prior to the formation of crystals. By contrast, atomic fluids, in which the motions are typically 11 orders of magnitude faster, cannot be compressed or quenched rapidly enough to achieve a glass state.

Naturally occurring glasses generally consist of aspherical molecules in which the suppression of rotation or the formation of bonded networks are dominant factors in preventing crystallization during supercooling of the fluid. On the other hand, the formation of the glass state in systems composed of spherical units, be they atoms or spherical particles, can only be associated with the suppression of translational motion. However, for systems of spherically interacting particles (eg. Lennard-Jones atoms and hard spheres) the only evidence for the existence of the glass state and its properties is contained in a considerable body of computer simulation and theory (for example Woodcock, 1981; Ullo and Yip, 1985; Bengtzelius, 1986). This work provides the following picture of the fundamental processes leading to the glass transition:

In the fluid phase ($\phi < \phi_F$) a typical particle or atom is able to diffuse throughout the sample although its progress is impeded by temporary entrapments in an

evanescent cage formed by neighboring particles. With increasing concentration, into the metastable fluid regime ($\phi_F < \phi < \phi_g$), the probability of a particle escaping from an increasingly compact neighbor cage decreases. As the glass transition is approached, the particle becomes essentially trapped in its cage but still retains some freedom to move within it.

The dynamics of systems of (near micron sized) colloidal particles can be determined by dynamic light scattering. This procedure is analogous to the inelastic scattering of neutrons by atomic fluids (Copley and Lovesey, 1975); the "contrast" of the scattering medium, which determines the relative proportion of coherent and incoherent scattering, can, for colloidal dispersions, be adjusted by altering the relative refractive indices of the particles. With suitably prepared dispersions, dynamic light scattering (DLS) allows measurement of the incoherent dynamic structure factor (van Megen and Underwood, 1989). This provides the statistical properties of the single particle displacement and allows the above picture of the particle motion in a fluid as the glass transition is approached to be tested directly. However, cessation of large scale translation of the particles, at the glass transition, must be accompanied by the partial "freezing-in" of concentration fluctuations on all spatial scales. Therefore, equally valuable insight into the nature of the particle dynamics around the glass transition is contained in the coherent dynamic structure factor. The latter expresses the decay of particle concentration fluctuations and, moreover, can be obtained by DLS on dispersions that are much more easily prepared than those required for incoherent scattering.

For a large number, N, of identical spherical particles in the scattering volume the (coherent) dynamic structure factor is defined by

$$F(q, \tau) = N^{-1} \sum_{j=1}^{N} \sum_{k=1}^{N} \langle \exp i\mathbf{q} \cdot [\mathbf{r}_j(\tau) - \mathbf{r}_k(0)] \rangle, \tag{4}$$

where $\mathbf{r}_j(\tau)$ is the position of particle j at time τ. $F(q, \tau)$ can also be expressed as

$$F(q, \tau) = \langle \rho(q, \tau) \rho^*(q, 0) \rangle \tag{5}$$

i.e. as the temporal autocorrelation function of the spatial Fourier component $\rho(q, \tau) = \sum_{k=1}^{N} \exp[i\mathbf{q} \cdot \mathbf{r}_k(\tau)]$ of the concentration fluctuations. Note that $F(q, 0) = S(q)$, the static structure factor defined by Equation (3).

The experimental arrangement and the procedure necessary to effect the ensemble average, indicated by the angular brackets in Equations (4) and (5), of the non-ergodic metastable states found near the glass transition are beyond the scope of this article and are presented elsewhere (Pusey and van Megen, 1987b). Here we focus the discussion on the measured coherent dynamic structure factors and their connection with the phase behavior of the dispersions in the vicinity of the glass transition.

The dispersions of pmma particles (of radius 170 nm) on which the discussion in this section is based, were also used for the static structure factor measurements discussed in Section 4. They exhibit a phase behavior similar to that described in Section 3 for dispersions of larger particles. The crystallization concentration was determined and, as discussed in Section 3, equated with the freezing volume fraction, ϕ_F, of the hard-sphere fluid. In terms of the effective hard-sphere volume fractions,

aspects of the phase behaviour of this dispersion, pertinent to this section, can be summarized as follows: Samples at volume fractions in the range $0.494 < \phi < 0.542$ crystallized within several hours after tumbling but the sample at a slightly greater volume fraction, $\phi = 0.554$ took several days to crystallize. In all these cases, crystallized within several hours after tumbling but the sample at a slightly greater observed for volume fractions in excess of 0.565, although, after several days, two samples at $\phi = 0.565$ and 0.582 showed some crystallization nucleated heterogeneously at their menisci. From this phase behavior we conclude that the glass transition is located at $\phi_g \simeq 0.560$. (It is not clear why this value of ϕ_g is somewhat lower than the value, $\phi_g \simeq 0.60$, found in the samples discussed in Section 3).

DLS measurements were performed on two equilibrium fluid-like samples at effective volume fractions $\phi = 0.480$ and 0.494; recall that the latter value equals ϕ_F, the effective hard-sphere volume fraction of the disordered phase that coexists with the crystalline phase (as seen, for example, in samples 3 to 5 in plate 1). Measurements were also performed on several samples at volume fractions $\phi > \phi_F$ after they had been extensively tumbled to obtain their metastable states. The light scattering measurements were made at a scattering angle corresponding to the position, q_m, of the main peak of the static structure factor, $S(q)$. In this choice we were guided by the availability of computer simulation data and theoretical predictions (Ullo and Yip, 1986; Bengtzelius, 1986). Physically, the wavelength $\lambda = 2\pi/q_m$, of the largest amplitude concentration fluctuations, is approximately equal to the mean interparticle spacing. In this sense the temporal decay of $F(q_m, \tau)$ represents a measure of the structural relaxation. Several features are evident from the results of $F(q_m, \tau)$ shown in Figure 3. Firstly, each of the dynamic structure factors has an initial decay noticeably faster than the long-time decay. In accordance with the above picture describing the particle dynamics, this rapid initial decay is associated with the local motion of the particles within their (average) neighbor cages, whilst the slower decaying component of $F(q_m, \tau)$ describes the more hindered particle diffusion over larger distances. Secondly, the time constant, T_L, of the slow decay increases much more rapidly with volume fraction than the time constant, T_s, of the initial fast decay. A detailed analysis of the data, (van Megen and Pusey, 1989), indicating that, $T_s \simeq 0.03$ sec. and varies only slightly over the volume fraction range ($0.480 < \phi < 0.582$) studied by DLS, but T_L varies from about 0.1 sec at $\phi = 0.480$ to 5 sec. at $\phi = 0.542$ and diverges for $\phi > 0.554$. This divergence of the decay time, T_L, evident from the non-decaying part of $F(q_m, \tau)$ shown in Figure 3, can be attributed to the spatial localization of the particles and the consequent partial freezing-in of concentration fluctuations of wavelength $2\pi/q_m$ at the glass transition. However, even when large scale motion has essentially ceased, the significant initial decay of $F(q_m, \tau)$ reflects the existence of some local motion of particles constrained or trapped in the amorphous glassy structure.

An important feature of these results is the correlation between the microscopic particle dynamics, as revealed by DLS, and the observed macroscopic phase behavior, summarized above. Samples at volume fractions $\phi < 0.542$ crystallized within several hours and their dynamic structure factors were roughly exponential at long times with decay times, T_L, less than about 5 sec. The lowest volume fraction sample

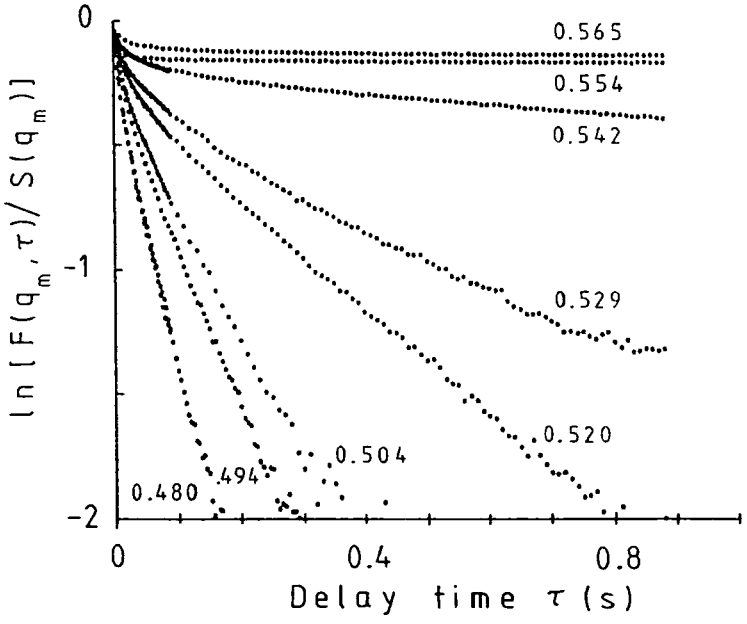

Figure 3 Dynamic structure factors, $F(q, \tau)$, for the metastable fluid states of the dispersions of the 170 nm pmma particles. The curves are labelled by effective hard-sphere volume fraction.

studied, $\phi = 0.554$, for which T_L diverged, took several days to crystallize. All samples studied a higher volume fractions showed a non-decaying component in $F(q_m, \tau)$; correspondingly, the metastable amorphous dispersions did not transform into a homogeneously nucleated crystalline phase over any period. Thus, the DLS measurements indicate the cessation of large scale particle motion at approximately the same volume fraction, $\phi_g \simeq 0.56$, at which the glass transition was located visually from the phase behavior.

Although the above results and discussion pertain to DLS measurements made only at $q = q_m$, the position of the primary maximum in $S(q)$, measurements were also performed at several other scattering vectors, both below and above q_m. At all values of q studied the dynamic structure factor displays a non-decaying component as ϕ_g is approached. This substantiates the assertion, made earlier in this section, that the suppression of large scale particle translation is accompanied by the partial freezing-in of concentration fluctuations of all spatial scales.

Quantitative comparison between the dynamic structure factors $F(q, \tau)$ measured on colloids and those obtained for atomic systems by theory and computer simulation is difficult due to the different natures of the particle motions in each case and the widely disparate timescales. Nevertheless we have devised a time-scaling procedure, based on diffusion times at the freezing concentration for each system, which leads to essentially quantitative agreement between our measurements of $F(q, \tau)$ and those calculated by Bengtzelius (1986) for Lennard-Jones atoms. Details of this comparison will be given elsewhere (van Megen and Pusey, 1989).

6 BINARY MIXTURES

Computer simulation techniques have been used extensively to study the freezing transition of single-component liquids (Frenkel and McTague, 1980), but so far no complete calculations have been made of the crystallization of binary fluids. This is not surprising since the properties of mixtures are much more varied and the phase behavior correspondingly more complex. Even a mixture of hard spheres, which may be viewed as conceptually the simplest model of a binary mixture, has three independent parameters (as opposed to one for the single-component case). The thermodynamics of a mixture of hard spheres of size ratio $\beta = R_B/R_A$ (we shall assume $R_A > R_B$ so $0 < \beta < 1$) may be described either in terms of the partial volume fractions

$$\phi_i = \frac{4\pi}{3} \rho_i R_i^3 \ (i = A \text{ or } B)$$

or the total volume fraction $\phi = \phi_A + \phi_B$ and the number fraction $x_A = \rho_A/\rho$, where ρ_i is the number density of component i and $\rho = \rho_A + \rho_B$.

Binary hard-sphere mixtures of all size ratios β are known to be completely miscible in the fluid phase (Alder, 1964; Lebowitz and Rowlinson, 1964). In contrast simple packing arguments suggest that the composition and structure of the equilibrium solid phase is determined primarily by the size ratio β. Density functional calculations predict that spheres of comparable diameters crystallize into substitutionally disordered close-packed structures (Barrat, Baus and Hansen, 1987). As the diameter ratio β decreases the degree of mutual solubility decreases and the phase diagram, presented as a function of temperature and number fraction at constant pressure, changes from a spindle shape to an azeotropic diagram and finally to a eutectic diagram (note that, as discussed in Section 3, experiments on colloidal systems are usually performed under constant volume conditions). At the most extreme size ratio reported of $\beta = 0.85$, the solid phase separation results in a pure close-packed crystal of small spheres and a substitutionally-disordered crystal containing largely big spheres. Mixtures of spheres with smaller size ratios might be expected to form ordered binary alloy structures. A simple free volume argument suggests that binary structures with touching close-packed densities in excess of the close packed volume fraction for monodisperse spheres of $\phi = 0.7405$ should be preferred at least at high pressures. It seems reasonable to expect that similar structures will be important at freezing even though the particles are not touching (see Section 4). Touching close-packed densities of a wide range of binary alloy structures have been calculated by Sanders and Murray (1980). With decreasing size ratio, the number of potential structures increases rapidly but for $\beta > \sqrt{2} - 1$ high-density close-packed binary alloys are found for size ratios of $\beta = 0.566$ (cubic AB_{13}, $\phi = 0.760$), $\beta = 0.527$ (hexagonal AB_2, $\phi = 0.782$) and $\beta = 0.414$ (cubic AB, $\phi = 0.793$). (Rather surprisingly, and in contrast to our findings below, recent density functional calculations (Rick and Haymet, 1989) of the freezing of 1:1 hard sphere mixtures predict that the stable solid phase at freezing for all size ratios is the substitutionally disordered FCC structure.)

The similarity of concentrated dispersions of pmma particles to hard sphere liquids makes them ideal candidates to test these ideas experimentally. In comparison with the rather limited range of diameter ratios found in atomic and molecular systems monodisperse colloidal spheres can be synthesised with a much wider range of mean diameters. Our most extensive set of measurements has been made on a system of size ratio $\beta = 0.61$. Both individual components, of radii of about 335 and 203 nm, showed phase behavior similar to that described in Section 3. As before the concentration at which crystallization of each component first occurred was identified with a hard sphere volume fraction of $\phi = 0.494$. All other volume fractions were scaled identically.

Binary dispersions were prepared at thirteen different number fractions x_A. At each composition, volume fractions ϕ were chosen so that the dispersion was in the vicinity of the equilibrium freezing line. The observed phase behavior was strongly dependent on the initial composition of the dispersion. Light scattering measurements identified four distinct solid phases corresponding to randomly stacked crystals of pure component A or component B, the ordered cubic binary alloy AB_{13} and a binary glass. The partial volume fractions of the dispersions in which each of these solid phases was observed is summarized in Figure 4. The dotted lines (of constant composition) separate samples which at equilibrium freeze into different solid structures.

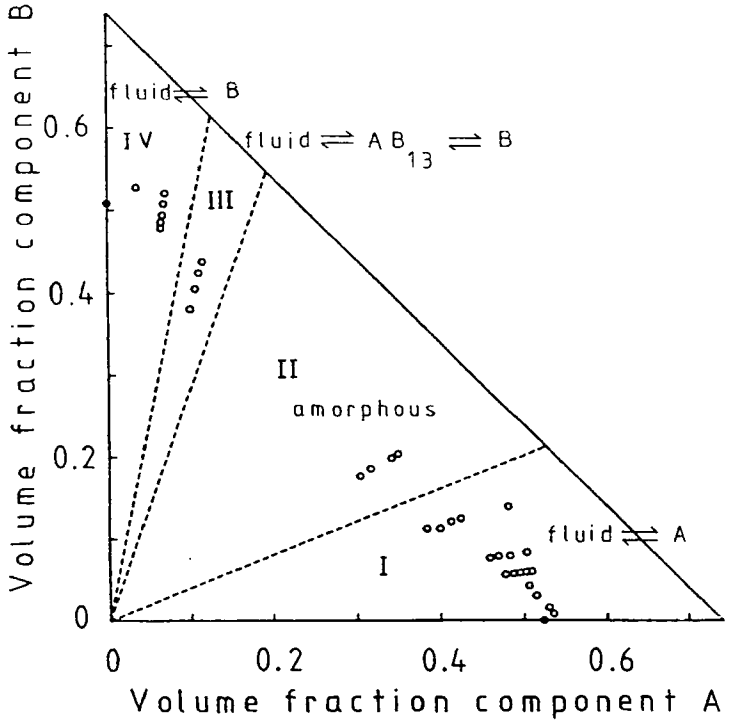

Figure 4 Constant volume phase diagram illustrating the binary dispersions investigated. The phase diagram is divided into four regions, I–IV, on the basis of the observed fluid-solid phase equilibria.

With increasing volume fraction, all binary dispersions of number fraction $x_A > 0.43$ (region 1 of Figure 4) separated into colloidal crystals and a coexisting binary fluid. Light scattering measurements together with scanning electron microscopy of dried crystalline samples showed that this crystalline phase consisted of large irregularly-stacked close-packed regions of component A with a similar structure to the crystals discussed in Section 4. Any occluded B spheres were present in amorphous grain boundaries consistent with almost total immiscibility of components A and B. Electron micrographs indicated that the solubility of component B in crystals of component A was less than 1 %. The coexisting fluid phase was correspondingly enriched in B particles. A similar degree of solid immiscibility was found for crystals formed from dispersions rich in component B of number fraction x_A less than 0.05 (region IV of Figure 4). In this region the phase separation resulted in a single crystalline phase containing component B and a coexisting fluid enriched in component A.

The most remarkable sequence of phase behavior occurred in the four samples with a number fraction $x_A \simeq 0.057$, containing approximately 17 small B spheres to 1 large A sphere. Crystallization was first observed in dispersions of total volume fraction $\phi = 0.511$ in which at equilibrium a single solid phase of irregularly stacked crystals of component B coexisted with a fluid phase. On increasing the volume fraction to $\phi = 0.535$ equilibrium was observed between three phases, one fluid and two solids. The diffraction pattern of the solid phase contained features characteristic of pure B crystals and also a regular progression of low q reflections implying a structure with a large lattice parameter. Detailed calculations (Bartlett, Ottewill and Pusey, 1989) demonstrate that the observed scattering intensity is consistent with powder diffraction from the ordered binary alloy AB_{13}. The structure of this compound can be considered in terms of a simple cubic subcell with A spheres at the cube corners. The cube contains a body-centred B sphere surrounded by twelve nearest neighboring B spheres at the vertices of a regular icosahedron. The unit cell is constructed from eight subcells with each adjacent icosahedral cluster rotated by $\pi/2$ about a simple cubic axis. On further increasing the volume fraction to $\phi = 0.554$ the binary dispersion crystallized totally into what appeared to be a single solid phase consisting of crystals of component B. No evidence was seen of a coexisting crystal phase of component A. Presumably the relatively small number of A particles were situated in amorphous grain boundaries.

With the observation of the binary crystal AB_{13} the phase diagram must contain at least three solid phases of A, B and AB_{13}. We might thus expect two eutectic points corresponding to the solid equilibria $B \rightleftharpoons AB_{13}$ and $A \rightleftharpoons AB_{13}$. The three coexisting phases seen in the sample of $x_A = 0.057$, $\phi = 0.535$ suggests that this sample lies in the eutectic region between B and AB_{13}. Dispersions prepared with a number fraction $x_A \simeq 0.28$ (region II of Figure 4), which might be expected to lie in the vicinity of the eutectic between A and AB_{13}, remained amorphous. Preliminary measurements by dynamic light scattering suggested binary glass formation. Since samples of comparable volume fractions but different compositions all readily crystallized we associate this composition with an enhanced tendency for glass formation. Glass formation at deep eutectics is commonly observed in other binary

systems such as metallic alloys. It has been attributed to the combined effect of an increased thermodynamic resistance to homogeneous nucleation at a eutectic and the kinetic restraints on crystal growth present in a binary mixture (Spaepen and Turnbull, 1984).

Unfortunately our data are not sufficiently complete to determine experimentally the full details of the phase diagram. In the absence of any theoretical predictions we have used a simple model for the freezing of binary hard spheres which predicts the form of the phase diagram under the conditions of constant volume relevant to our experiments. We model the system by a binary mixture of hard spheres, of size ratio β, which through miscible in the fluid phase are assumed to be totally immiscible in the solid phase. The experimental data, outlined above, suggest this is a reasonable approximation for dispersions of composition within the ranges $x_A > 0.43$ and $x_A < 0.05$. Using accurate equations of state for both the binary hard sphere fluid (Mansoori *et al.*, 1971) and the hard sphere single component crystal (Young and Alder, 1979) the densities of coexisting fluid and crystals may be readily determined. Figure 5 shows a section of the eutectic phase diagram in the partial volume fractions (ϕ_A, ϕ_B) plane calculated for a diameter ratio of 0.61.

In region (a) the binary fluid is the only stable phase, while in regions (b) and (c)

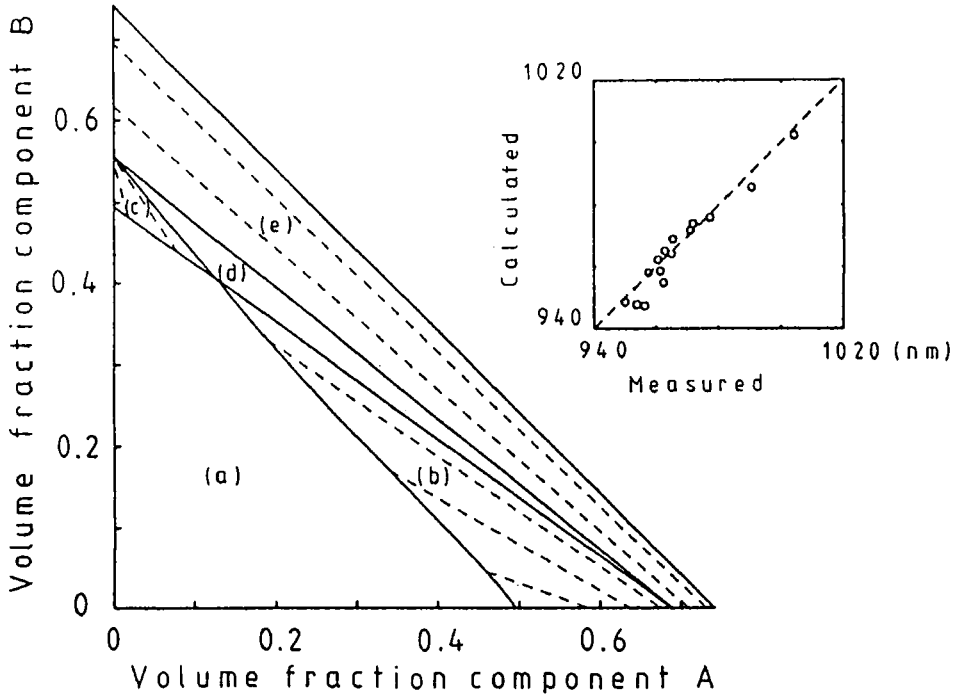

Figure 5 The ϕ_A, ϕ_B projection of the phase boundaries for the freezing of a binary hard sphere fluid into immiscible crystals. A diameter ratio of 0.61 has been assumed. Illustrative tie lines which connect coexisting states at constant osmotic pressure are shown dashed. On the inset diagram the predicted lattice parameters are compared with the experimentally determined lattice parameters found for crystals of component *A*.

the fluid is in equilibrium with a pure crystal phase. The states corresponding to the end of each tie line are the coexisting fluid and solid phases at a defined (osmotic) pressure. Each point on the tie line corresponds to the overall composition of the initial system which at equilibrium will phase separate into the states represented by the ends of the tie line. Samples prepared within region (d) will phase separate at equilibrium into three phases of eutectic fluid and crystals of A and B represented by the three vertices. Within this region the phase rule dictates that the equilibrium pressure is fixed. Finally in region (e) the system has totally solidified and crystals of A are in equilibrium with crystals of B. In practice the equilibrium states expected in regions (d) and (e) may not be achieved due to the intervention of glass transitions.

For dispersions rich in component A (region b of Figure 5) the osmotic pressure increases as the number fraction of the larger component is reduced and the total number density ρ increases. Coexisting crystals are correspondingly compressed. The subsequent change in the crystal density and hence the crystal lattice parameter predicted by the phase diagram of Figure 5 accurately mirrors the observed lattice parameters of crystals formed in the regions of solid immiscibility $x_A > 0.43$ and $x_A < 0.05$. The inset in Figure 5 shows the measured lattice parameters of crystals formed from binary dispersions of $x_A > 0.43$ against the predictions of the calculated phase diagram of Figure 5. Agreement is excellent and demonstrates that this simple model accurately predicts the phase behavior of dispersions rich in component A or component B.

In conclusion, these experiments demonstrate the complexities of colloidal binary hard sphere phase diagrams. In dispersions in which either the large or small components predominates we find that colloidal spheres at freezing are almost completely immiscible. In a very narrow range of intermediate compositions the ordered binary alloy phase AB_{13} is formed. Although the full details have still to be determined, the experimental evidence suggests that the phase diagram contains at least two eutectic compositions.

7 CONCLUDING REMARKS

We have described a variety of phenomena related to the phase behavior of one- and two-component dispersions of hard-sphere colloids. The analogy with the hypothetical hard-sphere atomic system has been emphasized. In several cases it has been possible to compare experimental results directly with theories and computer simulations applied originally to atoms.

We hope that future development of this program will continue to elucidate properties of simple materials in their fluid, crystalline and glassy states. For example, in view of the dominance of homogeneous nucleation, the slow growth rates and the possibility of observing the particles directly by light microscopy, these colloidal dispersions should constitute good models for further study of a simple freezing transition. Investigation of the behavior of binary mixtures of colloids, viewed as analogues of metallic alloys, should help to separate those properties determined largely by packing considerations from those which depend on detailed features of

the inter-atomic potential such as softness, attractions and directionality. In our study at just one size ratio we have already identified eutectics, glass formation and the colloid analogue of an intermetallic compound.

Acknowledgments

We thank R. H. Ottewill and S. M. Underwood for providing the particles, J. G. Rarity for constructing the light-scattering goniometer used for determining the crystal structure, B. J. Ackerson for assistance in interpreting the measured powder patterns and all four for useful discussions. We also thank D. W. Oxtoby for several valuable suggestions concerning the binary mixtures.

References

Alder, B. J. (1964) Molecular dynamics III mixture of hard spheres, *J. Chem. Phys.* **40**, 2724–2730.

Alfrey, T., E. B. Bradford, J. W. Vanderhoff and G. Oster (1954) Optical properties of uniform-particle-size lattices, *J. Opt. Soc. Am.*, **44**, 603–609.

Antl, L., J. W. Goodwin, R. D. Hill, R. H. Ottewill, S. M. Owens, S. Papworth and J. A. Waters (1986) The preparation of poly(methylmethacrylate) latices in non-aqueous media. *Colloids Surfaces*, **17**, 67–78.

Barrat, J. L., M. Baus and J. P. Hansen (1987) Freezing of binary hard-sphere mixtures into disordered crystals: a density functional approach. *J. Phys.* **C, 20**, 1413–1430.

Bartlett, P., R. H. Ottewill and P. N. Pusey (1989), *to be published.*

Bergtzelius, U. (1986) Dynamics of a Lennard-Jones system close to the glass transition. *Phys. Rev.* **A, 34**, 5059–5069.

Chaikin, P. M., J. M. di Meglio, W. Dozier, H. M. Lindsay and D. A. Weitz (1987) Colloidal Crystals in *Physics of Complex and Supermolecular fluids*, Eds. S. A. Safran and N. A. Clark, Wiley, N.Y.

Colot, J. L. and M. Baus, (1985) The freezing of hard spheres II. A search for structural (f.c.c.-h.c.p.) phase transitions. *Molec. Phys.*, **56**, 807–824.

Constantin, R, (1914) Osmotic compressibility of emulsions *Compt. Rend.*, **158**, 1171–1173.

Copley, J. R. D. and S. W. Lovesey (1975) The dynamic properties of monatomic liquids. *Rep. Prog. Phys.*, **38**, 461–563.

Edwards, O. S. and H. Lipson, (1942) Imperfections in the structure of Cobalt I. Experimental work and proposed structure. *Proc. Roy. Soc. (London)*, **A180**, 268–277 (277–285).

Egelstaff, P. A. (1967) *An Introduction to the Liquid State*, Fig 1b, *Academic Press, London.*

Einstein, A. The relevant papers published by Einstein between 1905 and 1911 have been translated into English by A. D. Cowper and edited by R. Furth, *The Theory of Brownian Movement*, Dover, 1956.

Frenkel, D. and A. J. C. Ladd (1984) New Monte Carlo method to compute the free energy of arbitrary solids. Application to the f.c.c. and h.c.p. phases of hard spheres. *J. Chem. Phys.*, **81**, 3188–3193.

Frenkel, D. and J. P. McTague (1980) Computer simulations of freezing and supercooled liquids. *Ann. Rev. Phys. Chem.*, **31**, 491–521.

Guinier, A. (1963) *X-ray Diffraction.* Freeman, N.Y.

Hansen, J. P. and I. R. McDonald (1976) *Theory of Simple Liquids*, Academic Press, New York.

Hendricks, S. B. and E. Teller (1942) X-ray diffraction in partially ordered layer lattices. *J. Chem. Phys.* **10**, 147–167.

Hess, W., and R. Klein (1983) Generalized hydrodynamics of systems of Brownian particles, *Adv. Phys.* **32**, 173–283.

Hiltner, P. A. and I. M. Krieger, (1969) Diffraction of light by ordered suspensions. *J. Phys. Chem.*, **73**, 2386–2389.

Hoover, W. G. and F. H. Ree (1968) Melting transition and communal entropy for hard spheres. *J. Chem. Phys.*, **49**, 3609–3617.

Igloi, F. {1986) Density functional theory of freezing of the hard sphere liquid into f.c.c. against h.c.p. structures *J. Phys., C*, **19**, 6907–6914.

Kirkwood, J. G. and F. P. Buff (1951) The statistical mechanical theory of solutions. *J. Chem. Phys.*, **19**, 774–777.

Klug, A., R. E. Franklin and S. P. F. Humphreys-Owen (1959) Crystal structure of Tipula iridescent virus as determined by Bragg reflection of visible light. *Biochem. Biophys. Acta*, **32**, 203–219.

Krieger, I. M. and F. M. O'Neill (1968) Diffraction of light by arrays of colloidal spheres. *J. Am. Chem. Soc.*, **90**, 3114–3120.
Langmuir, I. (1938) The role of attractive and repulsive forces in the formation of tactoids, thixotropic gels, protein crystals and coacervates. *J. Chem. Phys.*, **6**, 873–896.
Lebowitz, J. L., and J. S. Rowlinson (1964) Thermodynamic properties of mixtures of hard spheres. *J. Chem. Phys.*, **41**, 133–138.
Luck, W., M. Klier and M. Wesslau (1963) Bragg reflections with visible light on monodisperse synthetic plastic latices. *Ber. Bunsenges. Phys. Chem.*, **67**, 75–85.
Mansoori, G. A., N. F. Carnahan, K. E. Starling and T. W. Leland (1971) Equilibrium thermodynamic properties of the mixture of hard spheres. *J. Chem. Phys.*, **54**, 1523–1525.
McMillan, W. G. and J. E. Mayer (1945) The statistical mechanics of multicomponent systems. *J. Chem. Phys.*, **13**, 276–305.
Ottewill, R. H. and I. Livsey (1987) The imbibition of carbon disulphide by poly(methyl methacrylate) latex particles. *Polymer*, **28**, 109–113.
Perrin, J. (1914) Osmotic compressibility of emulsions considered as fluids of visible molecules. *Compt. Rend.*, **158**, 1168–1171.
Pusey, P. N. and W. van Megen (1986) Phase behaviour of concentrated suspensions of nearly hard colloidal spheres. *Nature*, **320**, 340–342.
Pusey, P. N. and W. van Megen (1987a) Properties of concentrated suspensions of slightly soft colloidal particles in *Physics of Complex and Supermolecular Fluids*. Eds. S. A. Safran and N. A. Clark, Wiley, N.Y.
Pusey, P. N. and W. van Megen (1987b) Observations of a glass transition in suspensions of spherical colloidal particles. *Phys. Rev. Letters*, **59**, 2083–2086.
Pusey, P. N., W. van Megen, P. Bartlett, B. J. Ackerson, J. G. Rarity and S. M. Underwood (1989) The structure of crystals of hard colloidal spheres, *Phys. Rev. Letters*, **63**, 2753–2756.
Rick, S. W. and A. D. J. Haymet (1989) Density functional theory for the freezing of Lennard-Jones binary mixtures. *J. Chem. Phys.*, **90**, 1188–1199.
Sanders, J. V. (1968) Diffraction of light by opals. *Acta Cryst.*, **A24**, 427–434.
Sanders, J. V. and M. J. Murray (1980) Close-packed structures of spheres of two different sizes II. Packing densities of likely arrangements. *Phil. Mag.*, **A42**, 721–740.
Spaepen, F. and D. Turnbull (1984) Metallic glasses. *Ann. Rev. Phys. Chem.*, **35**, 241–263.
Tough, R. J. A., P. N. Pusey, H. N. W. Lekkerkerker and C. van den Broeck (1986) Stochastic descriptions of the dynamics of interacting Brownian particles, *Molec. Phys.*, **59**, 595–619.
Ullo, J. J. and S. Yip (1985) Dynamical transition in a dense fluid approaching structural arrest. *Phys. Rev. Letters* **54**, 1509–1512.
van Megen, W. and I. Snook (1984) Equilibrium properties of suspensions. *Adv. Colloid Interface Sci.*, **21**, 119–194.
van Megen, W. and S. M. Underwood (1989) Tracer diffusion in concentrated colloidal dispersions III Mean squared displacements and self diffusion coefficients. *J. Chem. Phys.*, **91**, 552–559.
van Megen, W. and P. N. Pusey (1989) Dynamic light scattering study of the glass transition in a colloidal dispersion. *to be published.*
Williams, R. C. and K. M. Smith (1957) A crystallizable insect virus. *Nature*, **179**, 119–120.
Wilson, A. J. C. (1942) Imperfections in the structure of Cobalt. III. Mathematical treatment of proposed structure. *Proc. Roy. Soc. Lond.*, **A180**, 277–285.
Wilson, A. J. C. (1949) *X-Ray Optics*. Methuen, London.
Woodcock, L. V. (1981) Glass transition in the hard-sphere model and Kauzmann's paradox. *Ann. N. Y. Acad. Sci.*, **37**, 274–298.
Young, D. A. and B. J. Alder (1974) Studies in molecular dynamics XIII. Singlet and pair distribution functions for hard-disc and hard-sphere solids. *J. Chem. Phys.*, **60**, 1254-1267.
Young, D. A. and B. J. Alder (1979) Studies in molecular dynamics. XVII. Phase diagrams for "step" potentials in two and three dimensions. *J. Chem. Phys.*, **70**, 473–481.